THE LANCET
Microbe

Supplementary appendix 2

This appendix formed part of the original submission and has been peer reviewed. We post it as supplied by the authors.

Supplement to: Ehrlich HY, Somé AF, Bazié T, et al. Tracking antimalarial drug resistance using mosquito blood meals: a cross-sectional study. *Lancet Microbe* 2023; published online April 19. https://doi.org/10.1016/S2666-5247(23)00063-0.

Supplementary Materials

Tracking antimalarial drug resistance using mosquito blood meals: a cross-sectional study

Hanna Y. Ehrlich[1,2*+], Fabrice A. Somé[3+], Thomas Bazié[3], Cathérine Neya Ebou[3], Estelle Lotio Dembélé[3], Richard Balma[3], Justin Goodwin[3], Martina Wade[3], Amy K. Bei[3], Jean-Bosco Ouédraogo[1,3], Brian Foy[4], Roch K. Dabiré[3], Sunil Parikh[1]

[1] Yale University, Dpt. of Epidemiology of Microbial Diseases, New Haven, CT, USA, 06511
[2] One Health Institute, University of California at Davis, Davis, CA, 95616
[3] Institut de Recherche en Sciences de la Santé, Bobo-Dioulasso, Burkina Faso
[4] Colorado State University, Dpt. of Microbiology, Immunology, & Pathology, Fort Collins, CO, USA, 80521
[+] These authors contributed equally
[*] Corresponding author

This PDF file includes:

Supplementary Methods

Study design. We employed a two-stage cluster sampling design (Fig. S2). In the first stage, we sampled concessions proportionally to population size of each village sector; we refer to concessions as partially enclosed residential areas generally comprised of an extended family residing in multiple sleeping houses.[1] We used a random-walk procedure to select concessions within sectors.[2] Second stage sampling differed by survey: in the first survey in October 2018, we randomly selected one house within each concession to collect mosquitos and blood samples from all consenting individuals residing within that house; in the second and third surveys in March and September 2019, respectively, we halved the number of concessions and collected blood samples from all consenting individuals residing within all sleeping houses in those concessions. For those surveys (2 and 3), samples were collected in an average of 89% (227/255) of sleeping houses and for 83% (322/388) of individuals reported as residing within that concession. Surveys 1 and 3 were conducted between monthly SMC administrations, at least two weeks after the monthly deployment.

Brief questionnaires were administered to an adult resident to assess the demographic composition of the concession as well as antimalarial treatment/prevention behaviors. Blood-fed mosquitos were transported to a laboratory or holding facility within 1-3 hours post-collection, rendered immobile with Chloroform, and separated by genus according to established taxonomic keys.[3] Given that collections could exceed 50-100 mosquitos in a single house during peak times, we set a cutoff of ten mosquitos per sleeping house within each concession.

Ultrasensitive *Plasmodium falciparum* detection. Genomic DNA was stored in 70 µL elution buffer at -20°C. DNA samples were assessed for *P. falciparum* DNA were detected by quantitative PCR (qPCR) targeting the *var* gene acidic terminal sequence (*var*ATS).[4] Briefly, 6 µL of 1X Taqman Gene Expression Mastermix (Applied Biosystems, Waltham, Massachusetts, USA), 1 µL each of 0·8 µM forward and reverse primers, 0·5 µL of 0·4 µM probe, and 3·5 µL of parasite DNA were combined and run on the C1000 Touch thermal cycler with CFX96™ optical reaction module (Bio-Rad Laboratories, Hercules, California, USA). Samples with cycle threshold values targeting *var*ATS (Ct_{varATS})>42·5 were deemed negative; the threshold was set as such because of the predominance of low-density infections in community samples and in mosquito blood meals. At least 4 negative controls and 2 positive controls were included in each plate. Primer/probe sequences and cycling conditions are in Tables S1-S2.

Multiplicity of infection genotyping. Briefly, primary PCRs were prepared in triplex (*csp/cpp/msp7*) and singleplex (*cpmp*) reactions in a final volume of 15 µL with 3 µL gDNA, 0·25 µM of each primer pair, and 7·5 µL KAPA HiFi HotStart Ready Mix (Roche, Basel, Switzerland). Nested PCRs were prepared in singleplex with added 5′ linker sequences in a final volume of 15 µL with 4 µL DNA template (5 µl for *cpmp*), 0·25 µM of each primer pair, and 7·5 µL KAPA HiFi HotStart Ready Mix (Table S2, S3). Amplicon products were quantified using the Quant-it PicoGreen Assay (Thermo Fisher Scientific, Waltham, Massachusetts, USA) and normalized. All samples with Ct_{varATS} <40 were initially included; those displaying gel electrophoresis bands after the nested PCR were selected for subsequence library preparation. Illumina sequence adapters and sample-specific molecular indexes were added in a third round of PCR, performed as triplex (*csp/cpp/msp7*) and singleplex (*cpmp*) reactions in a final volume of 15 µL with 3 µL of template DNA, 0·67 µM adapter primer pairs, and 7·5 µL KAPA HiFi HotStart Ready Mix (Table S2, S3). Adapter PCR products were purified with NucleoMag beads (Macherey-Nagel, Düren, Germany), quantified, and combined into pools of equal concentration. The final sequence library was purified with NucleoMag beads, quantified by Qubit fluorometer (Thermo Fisher), and normalized. Sequencing was performed on an Illumina MiSeq platform in paired-end mode (2 × 300 bp) with Illumina MiSeq reagent kit v3 at the Yale Center for Genome Analysis (New Haven, Connecticut, USA).

Samples were analyzed using the bioinformatic pipeline HaplotypR.[5-7] Paired sequencing reads were demultiplexed by individual sample and gene marker, trimmed according to quality, and merged together. Mismatches were identified for each sample at each nucleotide position according to reference sequences (from PlasmoDB v·9·0 3D7) with SNPs requiring a >50% mismatch rate from ≥ 2 samples. Sequences were clustered using Swarm2 to predict haplotypes, and clusters with single haplotypes were

deemed as noise (singletons).[8] Potential chimeric reads were identified with vsearch.[9] HaplotypR then classified sequences as true haplotypes, singletons, chimeras, noise, or indels. True haplotypes required a minimum read coverage of three reads per sample and a within-host haplotype frequency of at least one percent. Samples with <25 reads per amplicon were excluded from the analysis. MOI was estimated as the maximum number of unique haplotypes identified at any of the four markers for each sample.

Antimalarial drug resistance genotyping with High Resolution Melting. Eluted DNA was enriched for HRM by multiplexed pre-amplification of samples, combining 5 µL of DNA, 10 µL of TaqMan PreAmp Master Mix Kit (Applied Biosystems) and 0·125 µM of each primer pair to a final volume of 20 µL. Asymmetric PCR reactions were performed using 2·5X LightScanner master mix (BioFire Diagnostics, Salt Lake City, Utah, USA), with each reaction including 1 µL of genomic DNA with forward primers at a concentration of 0·2 µM, reverse primers at 1 µM, and allele specific probes at 0·8 µM (Table S2, S3). LightCycler 96 Instrument (Roche) software was used to visualize normalized melting peaks of probes based on different melting temperatures, indicative of different base pairs, and compared with controls to verify genotypes for a given marker. Samples were initially assessed in duplicate and samples displaying no probe peak in three or more replicates were deemed inconclusive. Due to challenges in genotyping, all samples from the dry season (survey two) which amplified for *pfcrt* Lys76Th (K76T) were processed by Sanger sequencing (Keck Oligonucleotide Synthesis, New Haven, Connecticut, USA).

Lab considerations for low density infections. Both mosquito-based and community-based sampling are complicated by low density and asymptomatic infections, in which assays often operate near the limits of their sensitivity. Further, *Anopheles* mosquitos typically ingest only a few hundred parasites within a small volume of blood (1-3 µl).[10-14] Given the challenges of low density infections and the limited volumes of mosquito blood meal samples, we experimented with multiple assays to detect SNPs, taking into account cost, throughput, and sensitivity, all of which also factor into the potential scale up of xenomonitoring efforts. We assessed restriction fragment length polymorphism (RFLP), ligase detection reaction with fluorescent microspheres (LDR-FM), high resolution melting (HRM), and molecular inversion probes (MIPs).[15-18] For SNP identification of resistance-associated molecular markers, we ultimately selected a high resolution melting (HRM) assay due to its high sensitivity and low cost. However, samples required 1) pre-amplification of template DNA, 2) singleplex HRM reactions for each molecular marker, which were 3) run as 2-3 replicates, using up substantial amounts of extracted DNA, and 4) HRM products were often subsequently submitted for Sanger sequencing, all of which increased costs.[19] Even with these safeguards, genotyping success was strongly inversely associated with initial parasite density as inferred by Ct_{varATS} (95% CI $\mu_{failed} - \mu_{called}$ = 2·30, 3·51; p<0·0001). Samples may also be selectively pre-amplified based on initial parasite concentration, as estimated by Ct_{varATS} or other quantitative detection assays. Other highly sensitive SNP assays may also be useful, once validated, for xenomonitoring. For amplicon-based deep sequencing for MOI, we assessed four markers previously validated for use with low density infections (marker *ama-1* was excluded due to poor amplification following gel electrophoresis of nested PCR products).[7,20]

Statistical analyses. All analyses were conducted in R version 4·1·0. GEEs were fit using the geepack package; equivalence testing was carried out with the TOSTER package; and figures/maps were created using osmdata and ggplot2 packages.[21-28]

P. falciparum prevalence: Comparisons of Ct_{varATS} values by group were assessed using the Welch Two Sample t-test. We fit intercept-only logistic models in a Generalized Estimating Equations (GEEs) framework to determine the prevalence of infection to account for clustering of infections by concession and village sector, allowing for the calculation of robust standard errors with exchangeable working correlations, for each survey.[29] Prevalence estimates were estimated as the logistic function of the intercept coefficient for $p \in (0,1)$ and 95% CIs were calculated using standard errors. Models were fit separately for each survey.

Molecular marker analysis: Whereas the proportion (also sometimes referred to as prevalence) of molecular mutations is the number of specimens with mutant (often including mixed) genotypes out of the total number sampled, mutation frequency expresses the proportion of resistant clones in the parasite population. Although proportion/prevalence estimates cannot account for multiclonal infections, they remain the typical metric for molecular marker surveillance. However, in regions experiencing hyperendemic malaria transmission, including our study site, genotyping estimates are more accurate when accounting for multiclonal infections.[30] We used maximum likelihood models developed by Okell et al. (2017) that incorporated mean MOI estimates and assumed the detection likelihood of any given clone was set at 65% due to the magnitude of low parasite density infections.

Simulations for preferential biting. Heterogeneous exposure to mosquito bites, also known as preferential biting, is a well-characterized phenomenon that may have also played a role in our results. Known as the Pareto rule, many field studies (including those in Burkina Faso) have found that ~80% of blood-fed mosquitos feed on ~20% of available human hosts, although preferences for specific individuals may vary over time.[31-33] We assessed the potential impact of the Pareto rule by simulating 1,000 datasets of 100 households. In each iteration, we first generated household/concession data where molecular marker *x* was binomially distributed at varying true proportions ($\hat{p}_x$) among monoclonal *P. falciparum*-infected individuals (n=6). We specified sampling probabilities for each infected individual such that ~20% of individuals received ~80% probability of being sampled ("fed on") by mosquitos (n=10). We estimated the simulated prevalence of the mutation in humans (p_{x_h}) and mosquitos (p_{x_m}) for each simulation at the household/concession and community levels.

Simulations for multi-host blood feeding. Mosquitos may harbor parasites from feeding on multiple individuals in a single feeding session and/or gonotrophic cycle, due to interruptions in feeding, or they may have ookinetes/oocysts within midguts from prior blood feeds. Researchers in Burkina Faso and Zambia found that 15 and 19% of field-caught blood-fed *Anopheles* mosquitos, respectively, fed on more than one human host in a single gonotrophic cycle.[33,34] Additionally, *An. gambiae* and *An. funestus* gonotrophic cycles last ~2 days and mosquitos may seek out blood meals every 2-4 days, with studies finding that 1 in 5 *Anopheles* underwent ≥2 gonotrophic cycles and 1 in 16 survived for ≥4 cycles.[35] Recent evidence also suggests that additional blood meals, even on uninfected individuals, accelerate oocyst growth, which may increase the likelihood of observing oocysts from previous feeds in mosquito midguts.[36,37] Because oocysts take 10-12 days to develop and multiple feeding is relatively common, it is likely that some proportion of blood-fed mosquito midguts in our study contained clones from previous and interrupted blood feeds. To assess the potential impact of multiple feedings on our results, we generated household/concession data for 100 households where molecular marker *x* was binomially distributed at varying true proportions ($\hat{p}_x$) among monoclonal *P. falciparum*-infected individuals (n=6). In each simulation, mosquitos (n=10) randomly fed on (i.e. sampled) individuals within each household and then a variable proportion of those mosquitos fed again on the same set of individuals. We estimated the simulated prevalence of marker *x* in humans (p_{x_h}) and mosquitos (p_{x_m}) by averaging across all houses and over 1,000 simulations.

Supplementary Results and Discussion

Malaria prevalence. The number of infected humans and mosquitos were not meaningfully correlated in each concession but were modestly correlated at the level of the village sector (Fig. S4, ρ=0·18, p=0·032). Ct_{varATS} values for infected samples were highest in survey two for both humans and mosquitos, signifying lower parasite densities in the dry season, particularly in mosquitos (Table 2). Ct_{varATS} values were also significantly lower in infected humans than in blood meals (p<0·0001, mean Ct_{varATS}=36·0, 38·8 and SD=4·2, 5·1, respectively). All no-template controls were negative (Ct_{varATS}<45) by qPCR.

Those ages 10-15 and 15-20 years had the highest infection rates out of the number sampled, whereas children <5 years had the lowest infection rates in all surveys (Fig. S3). These results add to a growing body of literature documenting the large reservoir of parasites present in school-age children and adolescents, with longitudinal studies across SSA substantiating this epidemiological shift.[38-41] Those 5-18 years of age have historically received less attention in control campaigns (including ITN distributions) compared to those <5 years of age, and this age group is currently excluded from SMC in our study region.[40,42] Further, a recent global burden of disease analysis found that malaria was the leading cause of death in West and Central Africa in children 5-19 years of age.[43] In light of these developments, we urge policymakers to more directly target this important age group in malaria control efforts.

We observed discrepancies in *P. falciparum* infection rates over time and between hosts. As expected, rates were higher in humans than blood-fed mosquitos, likely due to mosquitos feeding humans with lower-density infections (i.e. those in the community rather than the clinic), feeding on non-human animals, and digestion or degradation of parasite DNA at the time of collection.[33] We also observed an unexpected decrease in malaria prevalence in humans over time. MOI also decreased over the three surveys, although the difference in the latter two surveys was not significant. We suspect that the decline in malaria may be related to a national piperonyl butoxide ITN campaign, distributed at our study site between the second and third survey, although we were unable to capture reliable ITN type and usage data in our study. Interestingly, mosquito blood meal infection rates responded only moderately to fluctuations in human infections, in line with recent work in southwest Burkina Faso and elsewhere which found that sporozoite rates remained constant across seasons.[44,45]

Molecular marker analysis. For marker *pfmdr1* Asn86Tyr (N86Y), we successfully genotyped 86·7% (210/242), 83·2% (119/143), and 89·2% (148/166) of 242 infected human samples and 89·5% (171/191), 94·5% (52/55), and 91·0% (91/100) of mosquito samples in surveys 1, 2, and 3, respectively. For marker *pfcrt* Lys76Th (K76T), we successfully genotyped 82·6% (200/242), 97·9% (140/143), and 85·6% (142/166) of human samples and 87·4% (167/191), 87·3% (48/55), and 96·0% (96/100) of mosquito samples in surveys 1, 2, and 3, respectively. Unsuccessful samples were distributed randomly across the study site and were unlikely to be indicative of systemic biases.

Simulations. Within individual households, we found that preferential biting behavior of *Anopheles* led to marked variability in the probability of observing mutant genotypes in mosquito blood meals. For genotypes circulating at high frequencies ($\hat{p}_x$=0·50), 40% of households had ≤10% or ≥90% mutant infections in mosquito midguts, compared to 0% in humans (Fig. S8). For mutant genotypes circulating at low frequencies ($\hat{p}_x$=0·050), most households (87·5%) possessed no mutant genotypes in any mosquito blood meals, and a small proportion of households (4·5%) had mutant genotypes in ≥70% of blood meals (Fig. S7). Empirically, for the molecular marker prevalent at lower frequencies (*pfmdr1* N86Y) throughout our study, we observed that 9/204 (4·4%) of concessions had ≥70% mixed/mutant infections in mosquito midguts and 187/204 (91·7)% had only wild-type infections in mosquito midguts.

Notably, however, when genotype prevalence was aggregated to the *community level* (calculated as the average mutation prevalence across all households), preferential biting did not lead to any significant differences in the mean prevalence or frequency of mutations between mosquitos and humans, regardless of the baseline mutation prevalence in the human population or the average host population MOI. However,

standard deviations for frequency and prevalence were consistently twice as large in mosquitos compared to humans (Fig. S8). Finally, when genotypes were aggregated to the community level without regard for household (calculated as the total number of mutant wild types out of the total individuals or mosquitos sampled) and when preferential biting only occurred within the greater community rather than in individual households, there was no observable difference between the prevalence/frequency or standard deviation of mutant genotypes in humans versus mosquitos.

For simulations for multi-host blood feeding, when all mosquitos fed twice, we found that the difference in p_x estimates in humans and mosquitos exceeded 10% as $\hat{p}_x$ approached 0·50. When 35% of all mosquitos fed twice, the magnitude of difference in p_x estimates decreased (Fig. S9).

Xenomonitoring feasibility and acceptability. Mosquito aspirations in each concession (mean=6·8 households) were generally completed within 15 minutes with a team of two to four entomology technicians. Nearly all adults surveyed (one per concession) expressed comfort with mosquito aspirations (152/153, 99·3%) as well as capillary finger pricks using lancets for themselves (148/153, 96·7%) and their children/dependents (142/153 92·8%). Participants mentioned research benefits and mosquito removal as the major benefits of aspiration, while others expressed doubt that removal would have substantial impact on malaria control as well as concerns relating to personal disturbance, particularly when sampling occurred very early in the morning. When comparing mosquito aspiration and finger pricks, 32·7% (50/153) did not have a preference between the two sampling methods. Of those with a preference, 39·8% (41/103) preferred finger pricks, citing that finger pricks can offer the possibility of rapid malaria diagnoses, and 60·2% (62/103) preferred aspiration.

Supplementary References

1. Turner AG, Magnani RJ, Shuaib M. A not quite as quick but much cleaner alternative to the Expanded Programme on Immunization (EPI) Cluster Survey design. *International journal of epidemiology.* 1996;25(1):198-203.
2. Levy PS, Lemeshow S. *Sampling of populations: methods and applications*: John Wiley & Sons; 2013.
3. Coetzee M. Key to the females of Afrotropical Anopheles mosquitoes (Diptera: Culicidae). *Malaria Journal.* 2020/02/13 2020;19(1):70.
4. Hofmann N, Mwingira F, Shekalaghe S, Robinson LJ, Mueller I, Felger I. Ultra-sensitive detection of Plasmodium falciparum by amplification of multi-copy subtelomeric targets. *PLoS medicine.* 2015;12(3):e1001788.
5. Lerch A. "HaplotypR". <https://github.com/lerch-a/HaplotypR>. Accessed March 30, 2022.
6. Lerch A, Koepfli C, Hofmann NE, et al. Development of amplicon deep sequencing markers and data analysis pipeline for genotyping multi-clonal malaria infections. *BMC genomics.* 2017;18(1):1-13.
7. Early AM, Daniels RF, Farrell TM, et al. Detection of low-density Plasmodium falciparum infections using amplicon deep sequencing. *Malaria journal.* 2019;18(1):1-13.
8. Mahé F, Rognes T, Quince C, de Vargas C, Dunthorn M. Swarm v2: highly-scalable and high-resolution amplicon clustering. *PeerJ.* 2015;3:e1420.
9. Rognes T, Flouri T, Nichols B, Quince C, Mahé F. VSEARCH: a versatile open source tool for metagenomics. *PeerJ.* 2016;4:e2584.
10. Smith RC, Vega-Rodríguez J, Jacobs-Lorena M. The Plasmodium bottleneck: malaria parasite losses in the mosquito vector. *Memórias do Instituto Oswaldo Cruz.* 2014;109:644-661.
11. Jeffery GM. Blood meal volume in Anopheles quadrimaculatus, A. albimanus and Aedes aegypti. *Experimental parasitology.* 1956;5(4):371-375.
12. Phasomkusolsil S, Pantuwattana K, Tawong J, et al. The relationship between wing length, blood meal volume, and fecundity for seven colonies of Anopheles species housed at the Armed Forces Research Institute of Medical Sciences, Bangkok, Thailand. *Acta tropica.* 2015;152:220-227.
13. Fauver JR, Weger-Lucarelli J, Fakoli III LS, et al. Xenosurveillance reflects traditional sampling techniques for the identification of human pathogens: A comparative study in West Africa. *PLoS neglected tropical diseases.* 2018;12(3):e0006348.
14. Grubaugh ND, Sharma S, Krajacich BJ, et al. Xenosurveillance: a novel mosquito-based approach for examining the human-pathogen landscape. *PLoS neglected tropical diseases.* 2015;9(3):e0003628.
15. Veiga MI, Ferreira PE, Björkman A, Gil JP. Multiplex PCR–RFLP methods for pfcrt, pfmdr1 and pfdhfr mutations in Plasmodium falciparum. *Molecular and cellular probes.* 2006;20(2):100-104.
16. Nankoberanyi S, Mbogo GW, LeClair NP, et al. Validation of the ligase detection reaction fluorescent microsphere assay for the detection of Plasmodium falciparum resistance mediating polymorphisms in Uganda. *Malaria Journal.* 2014/03/14 2014;13(1):95.
17. Ndiaye YD, Diédhiou CK, Bei AK, et al. High resolution melting: a useful field-deployable method to measure dhfr and dhps drug resistance in both highly and lowly endemic Plasmodium populations. *Malaria journal.* 2017;16(1):1-10.
18. Aydemir O, Janko M, Hathaway NJ, et al. Drug-resistance and population structure of Plasmodium falciparum across the Democratic Republic of Congo using high-throughput molecular inversion probes. *The Journal of infectious diseases.* 2018;218(6):946-955.
19. Daniels R, Hamilton EJ, Durfee K, et al. Methods to increase the sensitivity of high resolution melting single nucleotide polymorphism genotyping in malaria. *JoVE (Journal of Visualized Experiments).* 2015(105):e52839.
20. Gruenberg M, Lerch A, Beck H-P, Felger I. Amplicon deep sequencing improves Plasmodium falciparum genotyping in clinical trials of antimalarial drugs. *Scientific reports.* 2019;9(1):1-12.
21. Team RC. R: A language and environment for statistical computing. 2013.
22. Højsgaard S, Halekoh U, Yan J, Højsgaard MS. Package 'geepack'. *R package version.* 2016:1.2-0.2015.
23. Lakens D. Equivalence tests: A practical primer for t tests, correlations, and meta-analyses. *Social psychological and personality science.* 2017;8(4):355-362.
24. Lakens D, Lakens MD. Package 'TOSTER'. 2018.
25. Padgham M, Lovelace R, Salmon M, Rudis B. osmdata. *Journal of Open Source Software.* 2017;2(14).
26. Wickham H. ggplot2. *Wiley Interdisciplinary Reviews: Computational Statistics.* 2011;3(2):180-185.

27. Haklay M, Weber P. Openstreetmap: User-generated street maps. *IEEE Pervasive computing.* 2008;7(4):12-18.
28. OpenStreetMap. <https://www.openstreetmap.org>. Accessed October 15, 2021.
29. Floyd S, Sismanidis C, Yamada N, et al. Analysis of tuberculosis prevalence surveys: new guidance on best-practice methods. *Emerging Themes in Epidemiology.* 2013/09/28 2013;10(1):10.
30. Somé AF, Bazié T, Zongo I, et al. Plasmodium falciparum msp 1 and msp 2 genetic diversity and allele frequencies in parasites isolated from symptomatic malaria patients in Bobo-Dioulasso, Burkina Faso. *Parasites & vectors.* 2018;11(1):1-8.
31. Scott TW, Githeko AK, Fleisher A, Harrington LC, Yan G. DNA profiling of human blood in anophelines from lowland and highland sites in western Kenya. *The American journal of tropical medicine and hygiene.* 2006;75(2):231-237.
32. Woolhouse ME, Dye C, Etard J-F, et al. Heterogeneities in the transmission of infectious agents: implications for the design of control programs. *Proceedings of the National Academy of Sciences.* 1997;94(1):338-342.
33. Guelbéogo WM, Gonçalves BP, Grignard L, et al. Variation in natural exposure to anopheles mosquitoes and its effects on malaria transmission. *Elife.* 2018;7:e32625.
34. Norris LC, Fornadel CM, Hung W-C, Pineda FJ, Norris DE. Frequency of multiple blood meals taken in a single gonotrophic cycle by Anopheles arabiensis mosquitoes in Macha, Zambia. *The American journal of tropical medicine and hygiene.* 2010;83(1):33-37.
35. Ramirez JL, Barletta ABF, Barillas-Mury CV. Molecular mechanisms mediating immune priming in Anopheles gambiae mosquitoes. *Arthropod Vector: Controller of Disease Transmission, Volume 1*: Elsevier; 2017:91-100.
36. Shaw WR, Holmdahl IE, Itoe MA, et al. Multiple blood feeding in mosquitoes shortens the Plasmodium falciparum incubation period and increases malaria transmission potential. *PLoS pathogens.* 2020;16(12):e1009131.
37. Kwon H, Simões ML, Reynolds RA, Dimopoulos G, Smith RC. Additional feeding reveals differences in immune recognition and growth of Plasmodium parasites in the mosquito host. *Msphere.* 2021;6(2):e00136-00121.
38. Andolina C, Rek JC, Briggs J, et al. Sources of persistent malaria transmission in a setting with effective malaria control in eastern Uganda: a longitudinal, observational cohort study. *The Lancet Infectious Diseases.* 2021;21(11):1568-1578.
39. Färnert A, Yman V, Homann MV, et al. Epidemiology of malaria in a village in the Rufiji River Delta, Tanzania: declining transmission over 25 years revealed by different parasitological metrics. *Malaria journal.* 2014;13(1):1-12.
40. Nkumama IN, O'Meara WP, Osier FH. Changes in malaria epidemiology in Africa and new challenges for elimination. *Trends in parasitology.* 2017;33(2):128-140.
41. Mawili-Mboumba DP, Akotet MKB, Kendjo E, et al. Increase in malaria prevalence and age of at risk population in different areas of Gabon. *Malaria journal.* 2013;12(1):1-7.
42. Kombate G, Guiella G, Baya B, et al. Analysis of the quality of seasonal malaria chemoprevention provided by community health workers in Boulsa health district, Burkina Faso. *BMC health services research.* 2019;19(1):1-8.
43. Liu L, Villavicencio F, Yeung D, et al. National, regional, and global causes of mortality in 5–19-year-olds from 2000 to 2019: a systematic analysis. *The Lancet Global Health.* 2022;10(3):e337-e347.
44. Soma DD, Zogo BM, Somé A, et al. Anopheles bionomics, insecticide resistance and malaria transmission in southwest Burkina Faso: a pre-intervention study. *PloS one.* 2020;15(8):e0236920.
45. Epopa PS, Collins CM, North A, et al. Seasonal malaria vector and transmission dynamics in western Burkina Faso. *Malaria Journal.* 2019/04/02 2019;18(1):113.
46. Temu EA, Kimani I, Tuno N, Kawada H, Minjas JN, Takagi M. Monitoring chloroquine resistance using Plasmodium falciparum parasites isolated from wild mosquitoes in Tanzania. *The American journal of tropical medicine and hygiene.* 2006;75(6):1182-1187.
47. Mohanty A, Swain S, Singh DV, Mahapatra N, Kar SK, Hazra RK. A unique methodology for detecting the spread of chloroquine-resistant strains of Plasmodium falciparum, in previously unreported areas, by analyzing anophelines of malaria endemic zones of Orissa, India. *Infection, Genetics and Evolution.* 2009;9(4):462-467.

48. Mharakurwa S, Kumwenda T, Mkulama MA, et al. Malaria antifolate resistance with contrasting Plasmodium falciparum dihydrofolate reductase (DHFR) polymorphisms in humans and Anopheles mosquitoes. *Proceedings of the National Academy of Sciences.* 2011;108(46):18796-18801.
49. Mharakurwa S, Sialumano M, Liu K, Scott A, Thuma P. Selection for chloroquine-sensitive Plasmodium falciparum by wild Anopheles arabiensis in Southern Zambia. *Malaria journal.* 2013;12(1):1-6.
50. Mendes C, Salgueiro P, Gonzalez V, et al. Genetic diversity and signatures of selection of drug resistance in Plasmodium populations from both human and mosquito hosts in continental Equatorial Guinea. *Malaria journal.* 2013;12(1):1-13.
51. Sarma D, Mohapatra P, Bhattacharyya D, Mahanta J, Prakash A. Research Note Genotyping of chloroquine resistant Plasmodium falciparum in wild caught Anopheles minimus mosquitoes in a malaria endemic area of Assam, India. *Tropical biomedicine.* 2014;31(3):557-561.
52. Rattaprasert P, Chaksangchaichot P, Wihokhoen B, Suparach N, Sorosjinda-Nunthawarasilp P. Detection of putative antimalarial-resistant plasmodium vivax in Anopheles vectors at Thailand-Cambodia and Thailand-Myanmar borders. *Southeast Asian Journal of Tropical Medicine and Public Health.* 2016;47(2):182.
53. Sorosjinda-Nunthawarasilp P, Bhumiratana A. Ecotope-based entomological surveillance and molecular xenomonitoring of multidrug resistant malaria parasites in anopheles vectors. *Interdisciplinary perspectives on infectious diseases.* 2014;2014.
54. Conrad MD, Mota D, Musiime A, et al. Comparative prevalence of Plasmodium falciparum resistance-associated genetic polymorphisms in parasites infecting humans and mosquitoes in Uganda. *The American journal of tropical medicine and hygiene.* 2017;97(5):1576.
55. Smith-Aguasca R, Gupta H, Uberegui E, et al. Mosquitoes as a feasible sentinel group for anti-malarial resistance surveillance by Next Generation Sequencing of Plasmodium falciparum. *Malaria Journal.* 2019/10/17 2019;18(1):351.
56. Nkemngo FN, Mugenzi LMJ, Tchouakui M, et al. Xeno-monitoring of molecular drivers of artemisinin and partner drug resistance in P. falciparum populations in malaria vectors across Cameroon. *Gene.* 2022/05/05/ 2022;821:146339.

Supplementary Tables

Study	Site	Genetic markers (no. SNPs)	Mosquitos (no. pos.)	Collection method	Humans (no. pos.)	Design, e.g. no. houses, seasons
Temu et al. (2006)[46]	Bagamoyo, Tanzania	pfcrt (1) pfmdr1 (1)	Heads/ thoraxes (338)	CDC light traps, pyrethrum sprays, mouth aspirators	Not done	15 houses; 2 years
Mohanty et al. (2009)[47]	Orissa, India	pfcrt (1)	Heads/ thoraxes (45), abdomens (45)	CDC light traps, mechanical aspirators	Not done	4 sites
Mharakurwa et al. (2011)[48]	Macha, Zambia	pfdhfr (5)	Midguts (81); salivary glands (64)	Pyrethrum spray catches	DBS (169)	15 25-km^2 grids
Mharakurwa et al. (2013)[49]	Macha, Zambia	pfcrt (1)	Heads/thoraxes (62); Abdomens (81)	Pyrethrum spray catches	DBS (128)	Not specified
Mendes et al. (2013)[50]	Miyobo, Ngo-namanga, Equatorial Guinea	pfcrt (2) pfmdr1 (2) pfdhps (4) pfdhfr (4)	Whole body (275)	Not specified	DBS (302)	2 seasons; 2 villages
Sarma et al. (2014)[51]	North Lakhimpur, Assam, India	pfcrt (1)	Heads/thoraxes (3)	CDC light traps	Not done	3 villages; 2 houses/village
Rattaprasert et al. (2016)[52,53]	Kanchana-buri, Trat, Thailand	pvdhfr pfmdr1	Salivary glands (3)	Not specified	Not done	Not specified
Conrad et al. (2017)[54]	Tororo, Uganda	pfcrt (1) pfmdr1 (5) pfdhps (4) pfdhfr (4)	Thoraxes (162)	CDC light traps	DBS (162)	100 house cohort; infected humans and mosquitos paired w/in household vicinities/40 days
Smith-Aguasca et al. (2019)[55]	Palmeira, Mozambique	pfK13 (4) pfcrt (1) pfmdr1 (5) pfdhps (5) pfdhfr (5)	Whole body (122); heads/ thoraxes; abdomens	Mouth aspirators, miniature light traps	Not done	Not specified
Nkemngo et al. (2022)[56]	Cameroon	pfK13 (seq) pfmdr1 (3)	Abdomens (274); heads/ thoraxes (201)	Indoor aspiration, human landing catches	Not done	9 sites; no. surveys/seasons differed by site

Table S1. Summary of published studies that have assessed the prevalence of various antimalarial resistance markers in mosquito stages of field-caught mosquitos.

Assay	Target gene	Primer	Sequence
qPCR	*varATS*	Forward	CCCATACACAACCAAYTGGA
		Reverse	TTCGCACATATCTCTATGTCTATCT
		Probe	6-FAM-TRTTCCATAAATGGT-NFQ-MGB
HRM	*pfmdr1* N86Y	Forward	TTATTATTTATATCATTTGTATGTGCTGTATTATCAGG
		Reverse	CAGGAAACAGCTATGACATCATTGATAATATAAATTGTACTAAACCTATAGATACT
		Probe	GAACATGAATTTAGGTGATGATATTAATCC**GC****
	pfcrt K76T	Forward	GTAAAACGACGGCCAGTTTCTTGTCTTGGTAAATGTGCTCA
		Reverse	CAGGAAACAGCTATGACCGGATGTTACAAAACTATAGTTACCAAT
		Probe	GTGTATGTGTAATGAATAAAATTTTTG**AC****
AmpSeq PCR N1	*cpmp*	Forward	CGATACAGGACATATAGA
		Reverse	TTCAATAACATTTACTAGG
	csp	Forward	ATCAAGGTAATGGACAAG
		Reverse	ACTCAAACTAAGATGTGTTC
	cpp	Forward	TGTCTGAACCAAATTCAA
		Reverse	GAATTTGTCACATTTGATGA
	msp7	Forward	GTATTATCAAAGGTAAAGGCA
		Reverse	TTGCATAACTATAAACACCAT
AmpSeq PCR N2 with linker	*cpmp*	Forward	GTGACCTATGAACTCAGGAGTCCATAAGTCATTAAAATTTAT GGAT
		Reverse	CTGAGACTTGCACATCGCAGCCGTTACTATCAAGATCGTTAATATC
	csp	Forward	GTGACCTATGAACTCAGGAGTCAAATGACCCAAACCGAAATGT
		Reverse	CTGAGACTTGCACATCGCAGCGGAACAAGAAGGATAATACCA
	cpp	Forward	GTGACCTATGAACTCAGGAGTCCAAGTTCACTTTTGGGAAATG
		Reverse	CTGAGACTTGCACATCGCAGCATTACTACCTTTCAGCATATCCGA
	msp7	Forward	GTGACCTATGAACTCAGGAGTCATGAACAAGAGATATCAACACA
		Reverse	CTGAGACTTGCACATCGCAGCTTAAATTGTTCATGGTATTCCTTA
Amp Seq adapter		Forward	AATGATACGGCGACCACCGAGATCTACACTCTTTCCCTACACGACGCTCTTCCGATCTXXXXXXXX*GTGACCTATGAACTCAGGAGTC
		Reverse	CAAGCAGAAGACGGCATACGAGATCGGTCTCGGCATTCCTGCTGAACCGCTCTTCCGATCTXXXXXXXX*CTGAGACTTGCACATCGCAGC

Table S2. Primer/probe sequences. qPCR= quantitative PCR; HRM= high resolution melting; N1, N2= Nest 1, Nest 2; AmpSeq=amplicon-based deep sequencing. *XXXXXXXX = barcode/index. **=2-SNP mismatch probe block.

Assay	Target gene/ Step	PCR step	Temp (°C)	Time	Cycles
qPCR	*varATS*	Pre-incubation	50	2 min	1
		Initial denaturation	95	10 min	1
		Denaturation	95	15 sec	45
		Annealing & Elongation	55	1 min	
HRM	Pre-amplification	Initial denaturation	95	10 min	1
		Denaturation	95	15 sec	14
		Annealing & Elongation	60	4 min	
	pfcrt K76T	Pre-incubation	95	120 sec	1
		Denaturation	95	30 sec	45
		Annealing & Elongation	68	30 sec	
		Cooling	84	30 sec	1
		Cooling	4	NA	1
		Initial melt	40	5 sec	1
		Melt start	40	5 sec	
		Melt end	90	1 sec	
	pfmdr1 N86Y	Pre-incubation	95	120 sec	1
		Denaturation	94	30 sec	55
		Annealing	66	30 sec	
		Elongation	74	30 sec	
		Cooling	37	30 sec	1
		Cooling	28	30 sec	1
		Initial melt	40	5 sec	1
		Melt start	45	5 sec	
		Melt end	90	1 sec	
Amp Seq	Nest 1	Pre-incubation	95	3 min	1
		Denaturation	98	30 sec	20
		Annealing	54*/52**	15 sec	
		Elongation	72	45 sec	
		Cooling	72	2 min	1
		Cooling	4	NA	1
	Nest 2	Pre-incubation	95	3 min	1
		Denaturation	98	20 sec	10
		Annealing	55	15 sec	
		Elongation	72	45 sec	
		Denaturation	98	20 sec	10*/15**
		Annealing	62	15 sec	
		Elongation	72	45 sec	
		Cooling	72	1·5 min	1
		Cooling	4	NA	1
	Adapter	Pre-incubation	95	3 min	1
		Denaturation	98	20 sec	10
		Annealing	58	30 sec	
		Elongation	72	45 sec	
		Cooling	72	2 min	1
		Cooling	4	NA	1

Table S3. Cycling conditions. For AmpSeq, triplex (*) reactions include markers *cpp, csp,* and *msp7* and duplex (**) reactions include *cpmp* and *ama1*. Marker *ama1* was excluded from this analysis.

Survey	Age group (N)	Mean MOI (SD); N	p value	Marker Genotype	*pdmdr1* N86Y N (prop)	*pfcrt* K76T N (prop)
1	<10 years	3.5 (2.65); 4	0.64	WT	42/44 (0.91)	28/44 (0.64)
				Mixed	0/44 (0.00)	10/44 (0.23)
				Mut	4/44 (0.09)	6/44 (0.13)
	≥10 years	2.79 (1.72); 14		WT	102/108 (0.94)	77/98 (0.79)
				Mixed	2/108 (0.02)	14/98 (0.14)
				Mut	4/108 (0.04)	7/98 (0.07)
	<18 years	3.08 (1.56); 12	0.73	WT	90/94 (0.96)	63/90 (0.70)
				Mixed	0/94 (0.00)	20/90 (0.22)
				Mut	4/94 (0.04)	7/90 (0.08)
	≥18 years	2.67 (2.58); 6		WT	54/60 (0.90)	42/52 (0.80)
				Mixed	2/60 (0.03)	4/52 (0.08)
				Mut	4/60 (0.07)	6/52 (0.12)
2	<10 years	3.56 (2.01); 9	0.051	WT	37/38 (0.97)	12/45 (0.27)
				Mixed	1/38 (0.03)	19/45 (0.42)
				Mut	0/38 (0.00)	14/45 (0.31)
	0≥10 years	1.6 (1.34); 5		WT	77/81 (0.95)	18/96 (0.19)
				Mixed	1/81 (0.01)	48/96 (0.50)
				Mut	3/81 (0.04)	30/96 (0.31)
	<18 years	3.17 (1.99); 12	0.003	WT	64/68 (0.94)	16/79 (0.20)
				Mixed	2/68 (0.03)	38/79 (0.48)
				Mut	2/68 (0.03)	25/79 (0.32)
	≥18 years	1.00 (0); 2		WT	50/51 (0.98)	14/62 (0.23)
				Mixed	0/51 (0.00)	29/62 (0.47)
				Mut	1/51 (0.02)	19/62 (0.31)
3	<10 years	2.29 (1.38); 7	0.44	WT	28/37 (0.75)	28/36 (0.78)
				Mixed	8/37 (0.22)	4/36 (0.11)
				Mut	1/37 (0.03)	4/36 (0.11)
	≥10 years	1.77 (1.36); 13		WT	85/109 (0.78)	83/97 (0.86)
				Mixed	17/109 (0.16)	11/97 (0.11)
				Mut	7/109 (0.06)	3/97 (0.03)
	<18 years	1.8 (1.15); 15	0.44	WT	75/104 (0.72)	75/95 (0.79)
				Mixed	23/104 (0.22)	13/95 (0.14)
				Mut	6/104 (0.06)	7/95 (0.07)
	≥18 years	2.4 (1.95); 5		WT	38/42 (0.90)	36/38 (0.95)
				Mixed	2/42 (0.05)	2/38 (0.05)
				Mut	2/42 (0.05)	0/38 (0.00)

Table S4. Genotyping results for MOI and molecular marker proportions stratified by age group for each survey. For MOI, age data was missing for 5 samples. P values compare the population MOIs for each respective age group (<10 years and ≥10 years; <18 years and ≥18 years) and for each respective survey.

Marker	Survey	Sub-village code	N_h	N_m	Freq_h	Freq_m	TOST p-value	NHST p-value
pfmdr1 N86Y	1	A	16	19	0	0.02	0.0072	0.53
		B	21	24	0	0.07	0.31	0.17
		C	54	24	0.09	0.05	0.15	0.52
		D	15	27	0	0.03	0.011	0.39
		E	21	32	0.05	0.05	0.047	0.99
		F	7	8	0.2	0	0.75	0.19
		G	76	35	0.03	0	0.00040	0.11
	2	A	13	11	0.04	0	0.13	0.47
		B	8	4	0	0	<0.0001	1.00
		C	20	8	0.02	0	0.011	0.50
		D	42	12	0.04	0	0.011	0.22
		E	25	13	0	0	<0.0001	1.00
		F	7	2	0	0	<0.0001	1.00
		G	4	2	0	0	<0.0001	1.00
	3	A	17	23	0.08	0.07	0.12	0.97
		B	17	4	0.17	0.13	0.37	0.85
		C	21	5	0.21	0	0.89	0.019
		D	16	6	0.16	0.17	0.27	0.95
		E	33	4	0.05	0.25	0.92	0.077
		F	18	22	0.13	0.07	0.41	0.37
		G	27	27	0.17	0.08	0.68	0.093
pfcrt K76T	1	A	14	18	0.1	0.52	1.00	<0.0001
		B	21	25	0.15	0.34	0.77	0.12
		C	56	22	0.17	0.53	0.99	<0.0001
		D	14	24	0.16	0.25	0.44	0.54
		E	22	32	0.07	0.27	0.85	0.036
		F	7	8	0.07	0.36	0.84	0.13
		G	66	38	0.16	0.44	0.98	<0.0001
	2	A	18	10	0.53	0.89	0.96	0.018
		B	8	6	0.6	1	0.99	0.0050
		C	22	8	0.44	0.8	0.93	0.043
		D	56	12	0.67	0.68	0.27	0.95
		E	26	14	0.31	0.64	0.93	0.032
		F	7	2	0.84	1	0.68	0.24
		G	4	2	0.75	1	0.76	0.25
	3	A	17	22	0.26	0.25	0.12	0.94
		B	17	3	0.12	0	0.80	0.057
		C	19	6	0.06	0.10	0.34	0.75
		D	12	4	0.28	0.13	0.59	0.48
		E	27	6	0.06	0.09	0.31	0.73
		F	16	22	0.08	0.2	0.64	0.096
		G	28	29	0.02	0.04	0.024	0.74

Table S5. Genotype frequencies stratified by sub-village, randomly coded from A-G. P-values are color-coded based on significance of equivalence (rejection of TOST null with 10% equivalence margins) and of lack of difference (failure to reject the NHST null). Frequencies were calculated using average population estimates for MOI for each host and survey. Nh= sample size in humans; Nm= sample size in mosquitos; TOST=Two-One-Sided t-Tests; NHST= Null Hypothesis Statistical Test based on Fisher's exact z-test.

Marker	Equivalence margins (+/-)	Survey 1		Survey 2		Survey 3	
		TOST p-value	NHST p-value	TOST p-value	NHST p-value	TOST p-value	NHST p-value
***pfmdr1* N86Y**	**0.02**	0.31	0.60	0.49	0.12	0.83	0.30
	0.03	0.16	0.60	0.21	0.12	0.76	0.30
	0.04	0.064	0.60	0.057	0.12	0.67	0.30
	0.05	0.021	0.60	0.0091	0.12	0.48	0.30
	0.10	<0.0001	0.60	<0.0001	0.12	0.062	0.30
	0.15	<0.0001	0.60	<0.0001	0.12	0.0091	0.30
	0.20	<0.0001	0.60	<0.0001	0.12	0.00014	0.30
	0.25	<0.0001	0.60	<0.0001	0.12	<0.0001	0.30
***pfcrt* K76T**	**0.02**	1	<0.0001	0.99	0.028	0.59	0.64
	0.03	1	<0.0001	0.99	0.028	0.5	0.64
	0.04	1	<0.0001	0.99	0.028	0.41	0.64
	0.05	1	<0.0001	0.97	0.028	0.26	0.64
	0.10	0.99	<0.0001	0.82	0.028	0.032	0.64
	0.15	0.98	<0.0001	0.76	0.028	0.003	0.64
	0.20	0.87	<0.0001	0.67	0.028	<0.0001	0.64
	0.25	0.5	<0.0001	0.39	0.028	<0.0001	0.64

Table S6. Sensitivity analysis the margins of equivalence on the p-value of statistical tests, the Two-One-Sided t-Tests (TOST) to assess statistical equivalence and the Null Hypothesis Statistical Test (NHST) based on Fisher's exact z-test. In our study, a TOST p-value <0.05 resulted in a rejection the null equivalence hypothesis, suggesting the effect falls within the equivalence bounds/margins. An NHST p-value <0.05 resulted in a rejection of the null significance hypothesis, suggesting an effect exists in the study population.

Supplementary Figures

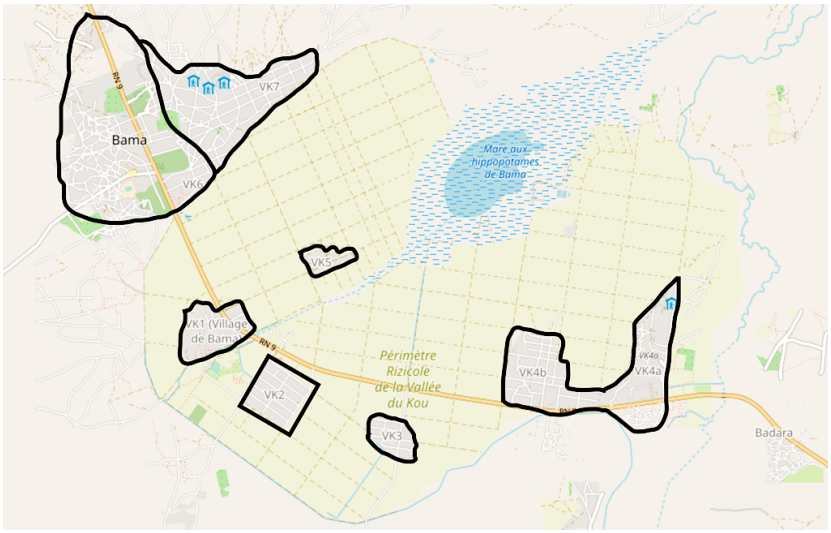

Figure S1. Study site of Bama in southwest Burkina Faso from OpenStreetMap. Map data copyrighted OpenStreetMap contributors and available from <https://www.openstreetmap.org>.[27,28] The seven sub-villages are outlined in black. Gray shading represents residential areas; yellow shading, rice cultivation; blue shading, water.

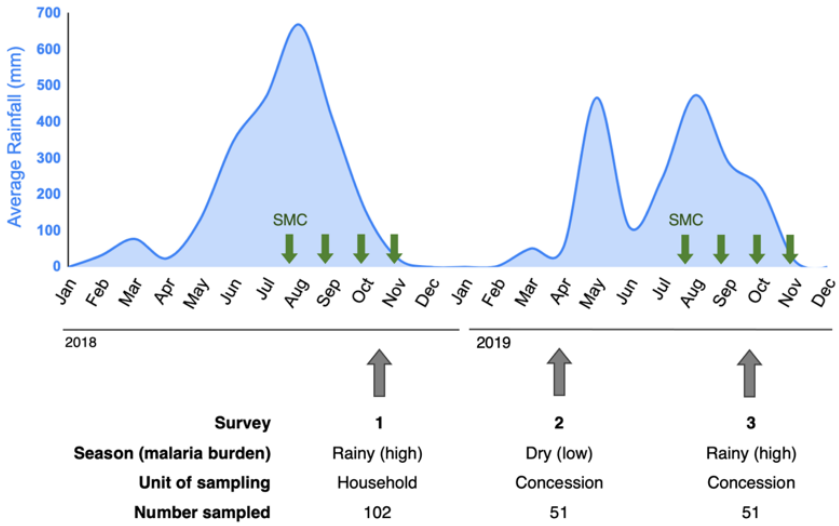

Figure S2. Sampling schema. Arrows correspond to the three cross-sectional survey dates, with respective concession-based sampling (single household per concession versus entire concession) information below each arrow. The graph displays the average rainfall (mm, blue shading) over the study period. SMC=seasonal malaria chemoprevention.

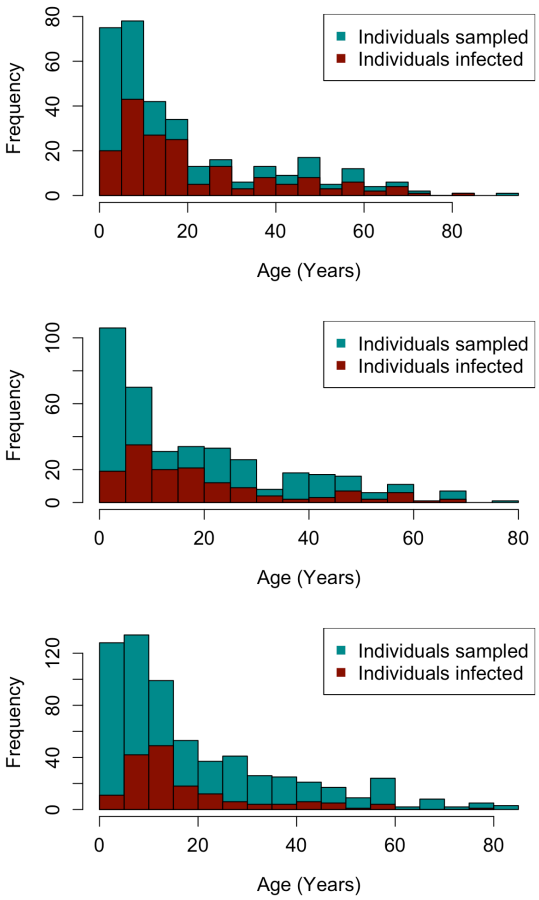

Figure S3. Ages of the number of individuals sampled (gray) versus infected (red), for surveys 1, 2, and 3 (top to bottom, respectively).

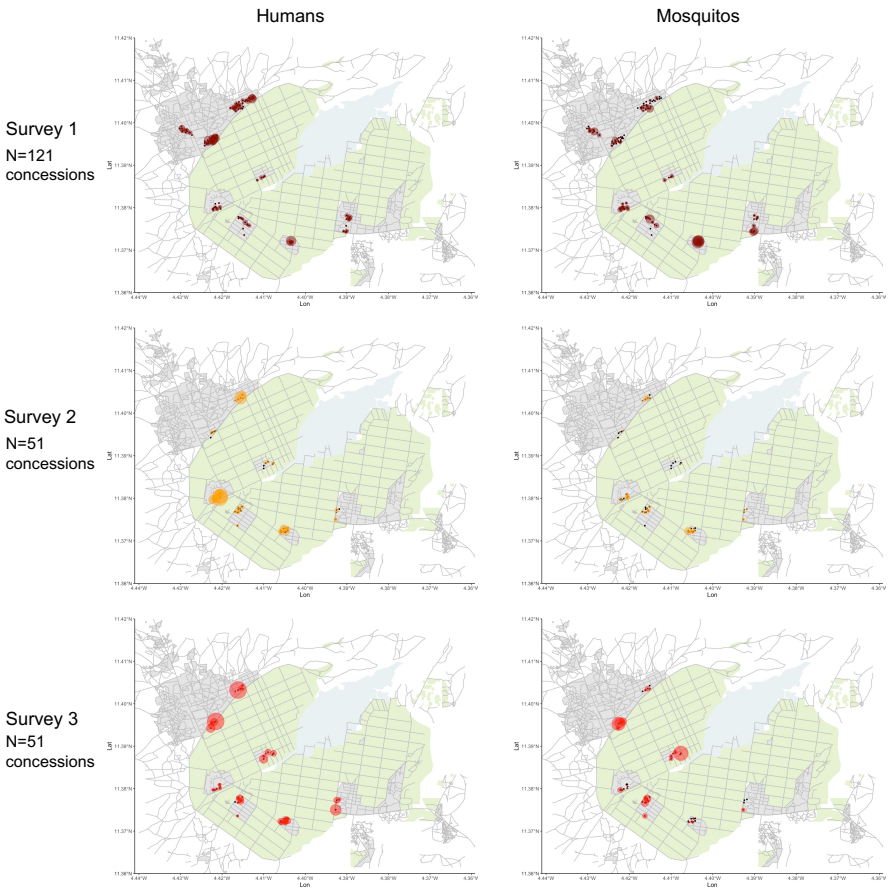

Figure S4. Comparison of number of individual humans and mosquitos infected per concession and survey for humans (left) and mosquito midguts/blood meals (right). Black dots correspond to concessions sampled. The size of the colored circles are proportional to the number of infected samples/specimens identified in each concession. All geographic coordinates are randomly jittered to protect anonymity. Maps adapted from OpenStreetMap.[27]

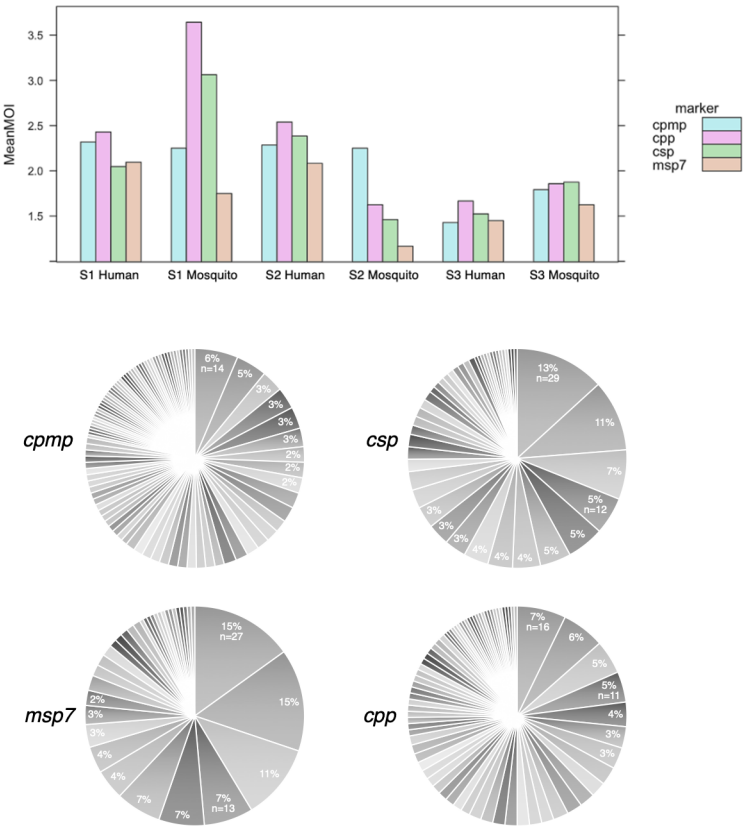

Figure S5. Bar plot (top) shows mean MOI estimates for each molecular marker, survey, and host (S=survey, H=humans, M=mosquitos). Mean MOI was calculated as the average maximum number of individual genotypes for each sample genotyped with Amp Seq within each subgroup. Slices in pie charts (bottom) demonstrate the number and percent of all genotyped samples across all surveys that contained a unique haplotype. For example, the most commonly identified *cpmp* haplotype was shared by 6% (n=14) of all samples.

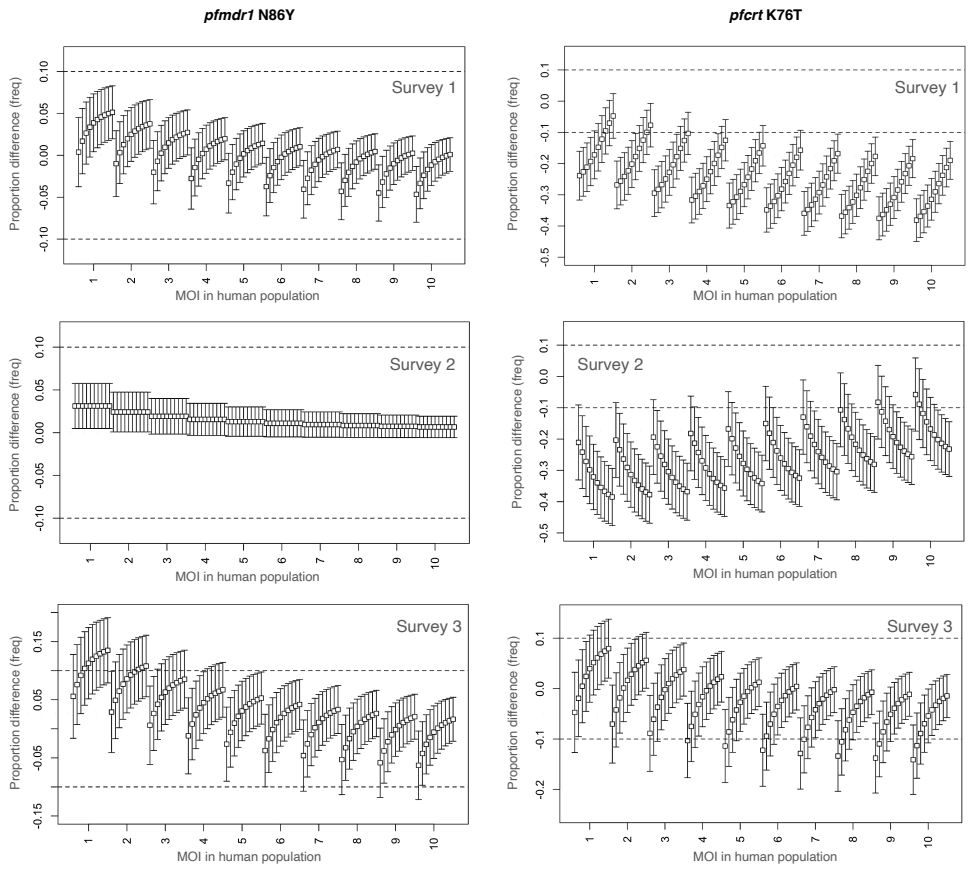

Figure S6. MOI sensitivity analysis to assess statistical equivalence of frequency estimates. For each value of MOI in the human population from 1 to 10 (x-axis), we varied the average MOI in the mosquito population from 1 to 10 (left to right). Frequency estimates were calculated by adjusting prevalence estimates for the respective MOI in each population and then compared using a statistical equivalence test based on Fisher's exact z-test. Boxes display the mean estimated difference in frequency between humans and mosquitos (i.e. the difference in the estimated frequency of mutant infections given our observed prevalence data for the marker in question), and whiskers show 95% confidence intervals. Dotted lines represent the margin of inferiority bounds (+/-10%) to assess the statistical significance of equivalence.

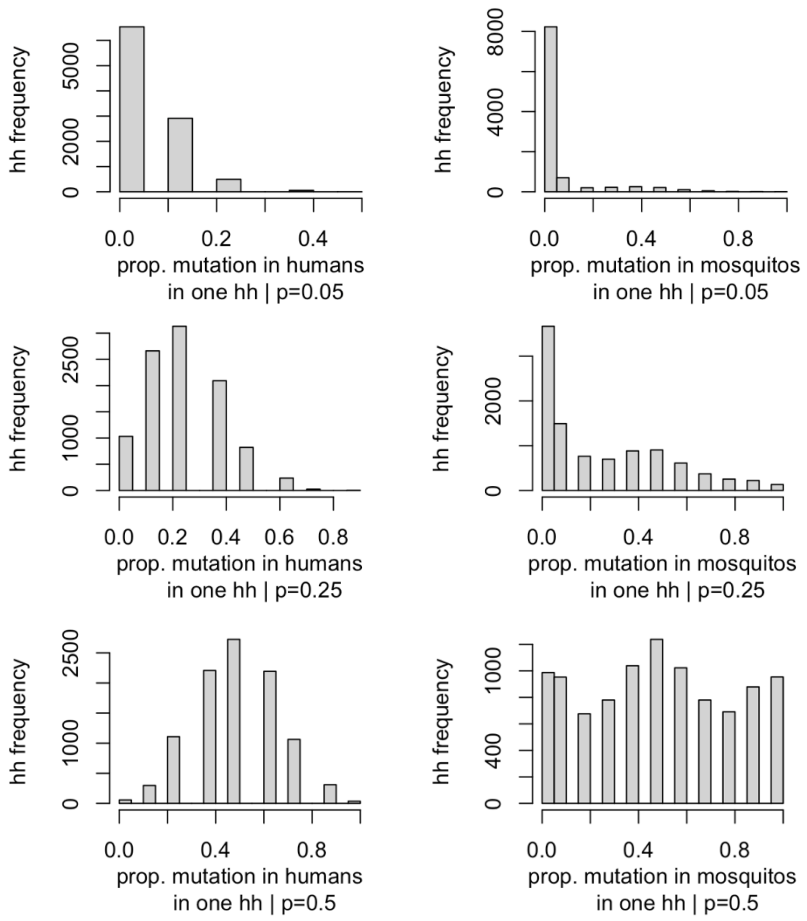

Figure S7. Histograms show the frequency of households (hh; y-axis) exhibiting a given proportion *p* of mutation *x* (x-axis) in either humans (left) or mosquito blood meals (right) over 100 simulations of 100 households, when the true population proportion of the mutation $\hat{p}_x$ in humans is either 0·05, 0·25 or 0·50 (top, middle, and bottom rows, respectively).

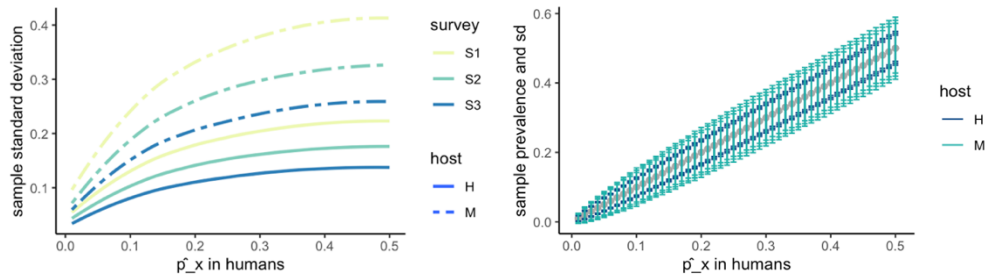

Figure S8. Preferential biting simulations wherein the mutation prevalence from simulated samples (p_x) and standard deviation (sd_x) are averaged across all households/concessions sampled. For each true population prevalence of the mutation in humans ($\hat{p}_x$), and for each survey design (S1, S2, and S3), we simulated the mutation status of people within individual concessions, randomly selected 20% of those individuals as those preferentially bit/sampled by mosquitos, and averaged the mean/standard deviations (SD) of all household prevalence estimates in humans (H) and mosquitos (M) to obtain the population prevalence, population SD (left) and 95% confidence intervals (right).

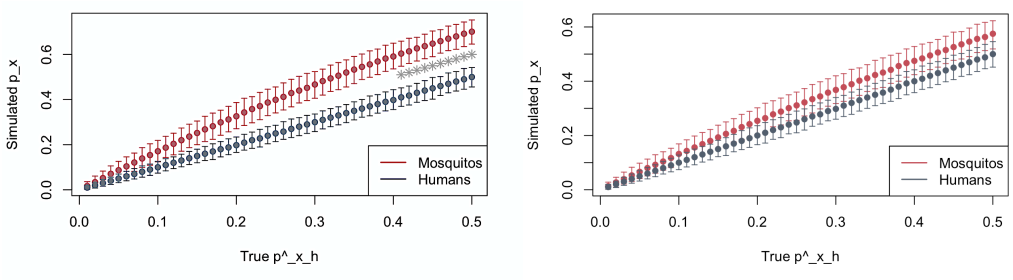

Figure S9. Multiple feeding simulations wherein the mutation prevalence from simulated samples (p_x) are averaged across all households/concessions sampled. For each true population prevalence of the mutation in humans ($\hat{p}_x$), we simulated the mutation status of infected individuals within households and allowed all mosquitos to feed twice on those Individuals (left) and 25% of mosquitos to feed twice on those individuals (right). Point estimates and 95% are displayed for humans [43] and mosquitos (red), and gray asterisks represent regions where the minimum difference in estimates exceeds 10%.